Space Flight Technology, German Space Operations Center (GSOC)
Deutsches Zentrum für Luft- und Raumfahrt (DLR) e.V.

Spaceborne GPS Receiver Performance Testing

O. Montenbruck, G. Holt

Doc. No. : TN 02-04
Version : 1.2
Date : May 9, 2002

Document Change Record

Issue	Date	Pages	Description of Change
1.0	April 13, 2002	all	First version
1.1	April 27, 2002	all	Minor updates
1.2	May 9,2002	all	Fixed specification for Test D4; updated Orion receiver description and test results for s/w version DLR61707I

Table of Contents

Scope

This report describes a generic test concept to assess the tracking performance of a spaceborne GPS receiver based on hardware-in-the-loop simulations. The test setup and configuration for a Spirent STR4760 GPS signal simulator are specified and the data analysis strategy is discussed. The test is specifically designed for low Earth satellite orbits but can be adapted to other dynamical conditions if required. Actual test results are provided for a Mitel Orion receiver adapted for space applications by DLR/GSOC.

1. Overview

1.1 Test Concept

To assess the tracking performance of a spaceborne GPS receiver, artificial GPS signals are generated which closely match the signals received by a spacecraft in low Earth orbit. The raw measurements and the navigation solution obtained by the receiver may then be compared against the simulated values. Other send a ground based testing with a roof antenna, the use of a signal simulator provides a realistic signal dynamics including high Doppler shifts and line-of-sight accelerations. In addition it allows the separate study of individual error sources (e.g. broadcast ephemeris errors or ionosphere) that may affect the quality of the resulting tracking data.

1.2 Simulation Scenario

The simulation is configured for a spacecraft orbiting the Earth in a near polar-orbit of 450 km altitude, 87° inclination, and an eccentricity of 0.005. The epoch, which coincides which the ascending crossing of the equator, is chosen as 6 Nov. 2001, 0:00 GPS Time, i.e. the beginning of day 2 of GPS week 1139. Consistent with this epoch the GPS constellation is modeled based on the actual GPS almanac for week 1138. Typically, all relevant test results can be collected in a simulation run of two hours.

1.3 Hardware Configuration

The subsequent test description is based on the use of a Spirent STR4760 GPS signal simulator [1] with one (or more) R/F outlet(s) and 16 single frequency (L1) channels. The choice of other simulator models or brands does not affect the basic test concept but may necessitate minor adaptations or restrictions. For testing dual frequency receivers, the simulator must be equipped with an L2 option and configured to generate P/Y code as desired.

To avoid stray radiation in the laboratory environment and achieve reproducible signal levels, the receiver is connected to the simulator's R/F output via shielded cables. The typical signal level generated by the receiver matches a value of –130 dBm corresponding to the signal strength sensed by a terrestrial antenna. Receiver's designed for use with active antennas (Orion, Pivot, SGR-xx, Mosaic) therefore require a low noise preamplifier of matching gain between the simulator outlet and the receiver antenna output. Other receivers with built-in preamplifier (BlackJack, GEM-S) can be connected directly to the simulator.

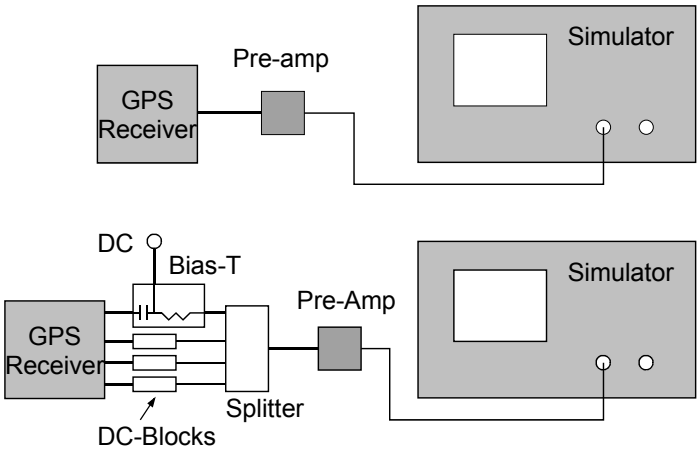

Fig. 1.1 Sample hardware setups for signal simulator testing of GPS receivers: use of preamplifier instead of active antenna (*top*) and test configuration for receiver with multiple antenna inputs using an external supply voltage for the pre-amplifier (*bottom*). DC carrying lines are indicated in bold.

Special attention may be required, if the receiver's antenna input pin does not supply an adequate DC power level (or none at all) for the external pre-amplifier. In this case the required voltage and current must be provided via a supplementary bias-T inserted between the receiver and amplifier. Attenuators (if required) should be placed between the simulator output and the preamplifier, i.e. in an non-DC carrying R/F line.

While the test is primarily designed to allow testing of individual receivers, power dividers can be used to simultaneously connect multiple receivers or antenna inputs to the simulator at the expense of a corresponding signal attenuation (3 dB for 2x splitters, 6 dB for 4x splitters). This may be useful for additional inter-receiver comparisons (zero-baseline test) or to provide equal signals to all antenna inputs of an attitude capable GPS receivers. At most one outlet of the power splitter is allowed to carry a DC supply voltage and proper DC blocks must be used if necessary. Sample test configurations are illustrated in Fig. 1.

2. Simulator Setup

The STR4760 simulator setup [1] is maintained in the form of configuration files, each covering a specific group of parameters (cf. Table 2.1). The root file (*.SCEN) provides a list of all configuration files that make up a particular scenario. It can be viewed with standard editors and printed for documentary purposes. With this exception, all configuration data are stored in binary files and should only be modified using the windows based configuration editors of the simulator software.

Table 2.1 Simulator configuration and output files

Directory	File	Format	Description
[.DATA]	LEO*.SCEN • LEO_NOERR.SCEN • LEO_EPH.SCEN • LEO_ION.SCEN • LEO_EPHION.SCEN	ASCII	Scenario root files • No intentional errors applied • with ephemeris errors • with ionosphere • with ephemeris errors and ionosphere
[.DATA]	LEO.SETUP	binary	Signal generator configuration (no. of r/f outputs, codes, etc.)
[.DATA]	YUMA114.DAT	ASCII	GPS Almanac in YUMA format for GPS week 1138 (=114+1024); used only upon creation of the GPS constellation definition (*.NAV_SAT)
[.DATA]	LEO*.NAV_SAT • LEO_NOERR.NAV_SAT • LEO_EPHERR.NAV_SAT	binary	GPS constellation definition (created from YUMA114.DAT), GPS-UTC difference • w/o ephemeris errors • with ephemeris errors
[.DATA]	LEO.SC_COM	binary	Common spacecraft parameters
[.DATA]	LEO*.SC_ION • LEO_NOION.SC_ION • LEO_20TECU.SC_ION	binary	Ionospheric refraction model • w/o ionosphere • with ionospheric delays
[.DATA]	LEO.ANT	binary	Antenna diagram
[.DATA]	LEO.SC_PER	binary	Spacecraft personality (mass, size, etc.)
[.DATA]	LEO.SC_REF	binary	Spacecraft orbit definition
[.RESULTS]	LEO*.*RTM	binary	Real-time data log
[.RESULTS]	LEO__ECEF.OCL	ASCII	Script for extraction of simulated s/c ephemeris
[.RESULTS]	LEO__PR.OCL	ASCII	Script for extraction of simulated pseudoranges
[.RESULTS]	LEO__PRR.OCL	ASCII	Script for extraction of simulated pseudorange rates
[.SCRATCH]	LEO_ECEF.CSV	ASCII	Simulated s/c ephemeris
[.SCRATCH]	LEO_PR.CSV	ASCII	Simulated pseudoranges
[.SCRATCH]	LEO_PRR.CSV	ASCII	Simulated pseudoranges

2.1 Scenario Definition

The scenario definition file (*.SCEN) acts as a root file for the description of the simulation setup. Besides holding a list of all elementary configuration files required by the scenario, it also defines the start time

6 Nov. 2001, 0:00:00 GPS Time

and maximum duration (86400 s) of the scenario. As indicated in Table 2.1, specific test configurations can be directly activated by choosing one of several predefined scenario definitions.

A single vehicle simulation is selected and the vehicle type is chosen as “spacecraft”. This allows the specification of spacecraft motion parameters and the application of alternate ionosphere models for high altitudes.

2.2 System Setup

The *.SETUP file defines the allocation of signal generators to frequency bands (L1 or L1/L2) and R/F outputs (one or more) of the simulator. In the standard test configuration 16 channels of L1 C/A(+P) code on a single R/F output are assumed. For dual frequency receiver testing, 16 channels of L1 & L2 (C/A+)Pseudo-Y code are recommended. The choice of Pseudo-Y code (versus P code) provides a more realistic simulation of the actual signal under Anti-Spoofing (A/S) conditions and may result in a different receiver performance than a simulation based on P-code. Since various receivers are known to distinguish between P code tracking and Y-code tracking based on the value of the Anti-Spoofing flag (bit 19 of the hand-over-word (HOW) in the GPS navigation message), it is strongly advisable, however, to ensure a consistent setting of this flag in the GPS constellation setup (cf. Sect. 2.3). If required, the test can also be performed on a 10 channel signal simulator (e.g. STR2760) with a moderate loss of information. In this case the minimum elevation of simulated satellites should be set to 5° in the constellation setup.

2.3 GPS Constellation

The GPS constellation definition stored in the *.NAV-SAT configuration files is based on a YUMA almanac describing the true constellation for GPS week 1138 (=114) and reference epoch t_{oa}= 589824 s (i.e. approximately 2.2 days before the simulation epoch). It comprises a total of 28 healthy satellites (all PRNs except 12, 16, 19, 32). For further reference a complete listing of the employed almanac file (YUMA114.DAT) is given in the annex. It can be imported into a GPS constellation file using the “Read and Write YUMA Almanac Data File” menu.

Satellite Selection

The simulator is configured to generate GPS signals for all satellites above a 5° obscuration angle measured from the Earth tangent. Satellites are selected based on a PDOP criterion using sequential replacement and 30s sampling.

An appropriate entry is made in the “General Control Details” menu.

GPS-UTC Difference

The GPS constellation file also specifies the difference between GPS and UTC time as part of the “General Control Details” menu. In accord with the actual offset for the considered epoch, a value of

GPS–UTC=13 s

has been adopted for the present simulation.

Other General Control Details

In addition to the above parameters the following settings are chosen in the “General Control Details” menu:

Clock & Ephemeris Divergence	Disabled
Signal Strength	Modeled
Clock Noise	Disabled
L1-L2 Delay	Modeled
Tropospheric refraction	Disabled

Parameters not mentioned are of no significance for the conducted simulations (**TBC**).

Signal Strength

By default, the simulator generates a GPS signal strength compatible with the minimum signal level specified for the GPS system in [2] (ca. –130 dBm for satellites at a mean distance from the observer) and a 0 dB vertical antenna gain. The overall signal level may, however, be adjusted to account for the actual antenna gain (ca. 3-5 dB in the boresight direction) as well as the actual GPS signal strength (ca. <3 dB above specification). In addition, a higher than normal signal level is required to compensate for the higher noise temperature experienced in simulator testing compared to the usual antenna sky temperature [3]. A software signal amplification of about 8 dB is therefore recommended to reproduce the signal strengths observed in open-air receiver tests. The amplification can be configured in the Satellite Signal Control Parameters window for each individual PRN or changed a run-time in the Real-Time Simulation – Antenna Details window. The antenna diagram itself is specified in the *.ANT configuration file (cf. Sect. 2.6)

Ephemeris Errors

Intentional ephemeris errors have been added as part of the LEO_ERR.NAV_SAT configuration file based on the maximum observed offsets between GPS broadcast ephemerides and precise IGS ephemerides for the simulation date (cf. [4], Table 2.2).

Table 2.2 Intentional broadcast ephemeris errors (ECEF system) applied in LEO_ERR.NAV_SAT

PRN	Δx [m]	Δy [m]	Δz [m]	PRN	Δx [m]	Δy [m]	Δz [m]
1	-6.5	3.7	-3.9	17	3.6	-2.5	4.0
2	4.1	-6.2	3.9	18	3.3	3.0	-2.6
3	4.2	5.0	3.9	20	-5.3	4.9	1.7
4	2.4	-1.8	3.2	21	-4.2	11.1	8.5
5	-2.6	-5.9	3.5	22	4.1	4.9	-5.2
6	7.2	-12.4	11.0	23	9.0	11.6	12.0
7	3.0	-2.6	1.9	24	-3.5	-5.9	-2.7
8	3.6	-5.6	3.4	25	7.0	7.2	-4.7
9	2.4	-5.0	-2.7	26	-1.6	1.7	-3.8
10	2.9	-4.0	-6.0	27	2.6	1.4	-1.7
11	-2.3	-3.3	-3.1	28	2.4	-1.8	-1.2
13	1.8	2.7	1.8	29	-5.4	7.3	-6.3
14	3.6	-4.1	-4	30	6.7	-4.3	6.5
15	-2.2	-2.9	1.9	31	2.5	-2.0	2.0

It is noted that the activation of broadcast ephemeris errors affects only the estimated receiver position but has virtually no impact on the velocity component of the navigation solution.

Anti-Spoofing Flag

For test of dual frequency receivers (e.g. BlackJack) or P-code capable single frequency receivers (e.g. GEM-S) the navigation data message should be modified to activate the anti-spoofing flag by setting bit 19 of the hand-over-word (=word number 2) to “1” for all simulated GPS satellites, subframes and pages. No dedicated configuration file is provided and the user is advised to check – and if necessary modify – the corresponding settings in the “Modify Nav Data” menu of the GPS Constellation File editor prior to starting a simulation.

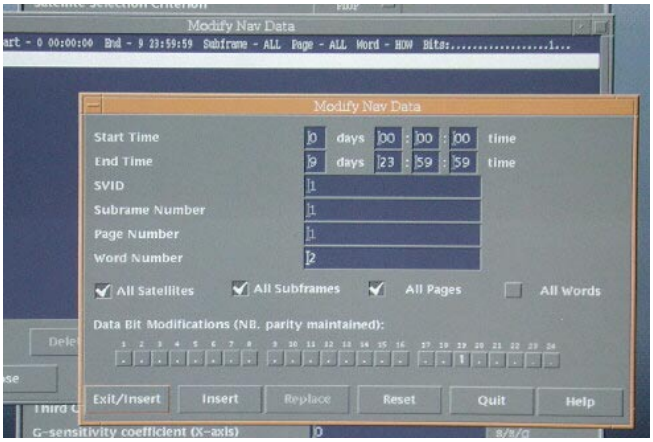

Fig. 2.1 Simulator setting for activating the Anti-Spoofing flag in the hand-over words of the GPS navigation data message

Ionospheric Data

The Klobuchar coefficients incorporated into the navigation message are specified in the “Ionospheric Data” menu of the GPS Constellation File editor. Values used in the simulation are summarized in Table 2.3. They are not designed to match the actually applied ionospheric path delay but may be used to check, whether ionospheric corrections are properly disabled in a spaceborne single frequency receiver (**TBC**).

Table 2.3 Klobuchar model coefficients for ionospheric refraction correction

Parameter	Value	Parameter	Value
α_0	$9.2 \cdot 10^{-9}$ s	β_0	87000 s
α_1	$1.8 \cdot 10^{-8}$ s/smc	β_1	50000 s/smc
α_2	$-7.2 \cdot 10^{-8}$ s/smc^2	β_2	-160000 s/smc^2
α_3	$-1.2 \cdot 10^{-7}$ s/smc^3	β_3	-330000 s/smc^3

2.4 Ionospheric Characteristics

The application of ionospheric path delays (and a corresponding carrier phase advance) is controlled by the Spacecraft Ionosphere and Earth Noise Models Editor. While the LEO_NOERR.SC_ION configuration file describes a ionosphere free simulation, a constant total electron content (TEC) of $2 \cdot 10^{17}$ electrons/m^2 (=20 TECU) is modeled in the LEO_ERR.SC_ION configuration. In both cases the SPACE ionosphere model is selected and Earth noise is deactivated.

2.5 Spacecraft Parameters and Trajectory Definition

The modeled spacecraft is assumed to fly in a 450 km altitude near circular, polar orbit, which resembles that of the Champ and Grace satellites. Detailed orbital elements and the corresponding ECEF epoch state vector are given in Table 2.3. The orbit is propagated by the simulator using a 10 x 10 gravity model and perturbations and the spacecraft attitude is specified as Earth pointing. Corresponding configuration data are specified in the spacecraft reference file (*.SC_REF) using the Spacecraft Initial Position File editor.

Table 2.3 Simulated spacecraft orbit

Epoch	2001 Nov. 05, 23:59:57 UTC 2001 Nov. 06, 00:00:00 GPS; GPS week 1139, 172800 s				
Elements (B1950)	Value	State vector (ECEF)		Value	
Semi-major axis (*a*)	6823.0 km	Position	*x*	33243.09	m
Eccentricity (*e*)	0.001		*y*	6816095.93	m
Inclination (*i*)	87.0°		*z*	174.18	m
Long. of ascend. node (Ω)	135.0°	Velocity	v_x	96.81065	m/s
Arg. of perigee (ω)	0.0°		v_y	-0.66740	m/s
Mean anomaly (*M*)	0.0°		v_z	7640.47705	m/s

For initialisation of the Orion GPS receivers, the resulting trajectory has been fit to the SGP4 orbit model, resulting in the set of NORAD twoline elements shown in Table 2.4.

Table 2.4 Twoline elements corresponding to the simulated spacecraft trajectory specified in Table 2.3

```
1 12345U 01999  A 01309.99984954 -.00020228  00000-0 -46117-3 0    04
2 12345  87.0008 134.9419 0012185 296.6516  63.3393 15.42601037    09
```

Supplementary to the orbital parameters specified above, the spacecraft personality file (*.SC_PER) specifies the ballistic properties of the satellite (A=1 m^2, m=1 ton, C_D=2.3) as well as the number (=1) and location of antennas (zero COG offset).

Finally an empty spacecraft motion file (*.SC_COM) is used to describe a maneuver free trajectory.

2.6 Antenna Diagram

An axis-symmetric, near hemi-spherical antenna diagram is assumed in the simulation. Attenuation values are specified on a 5° elevation grid relative to the vertical sensitivity within the configuration file LEO.ANT.

Table 2.5 Hemispherical antenna gain pattern LEO.ANT (normalized to vertical gain 0 dB)

E [°]	G [dB]	E [°]	G [dB]	E [°]	G [dB]	E [°]	G [dB]
87.5	-0.0	62.5	-0.5	37.5	-2.2	12.5	-6.6
82.5	-0.0	57.5	-0.7	32.5	-2.7	7.5	-8.9
77.5	-0.1	52.5	-1.0	27.5	-3.4	2.5	-13.6
72.5	-0.2	47.5	-1.3	22.5	-4.2	-2.5	-40.0
67.5	-0.3	42.5	-1.7	17.5	-5.2	-7.5	-40.0

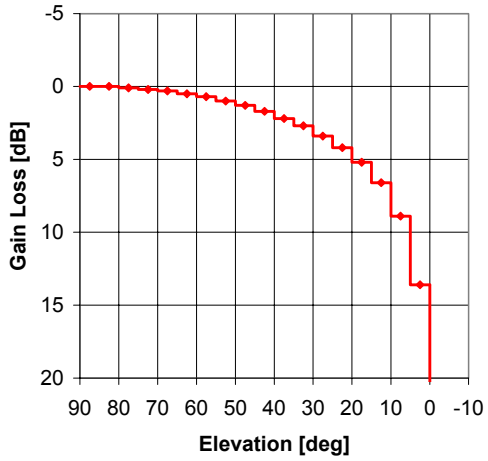

Fig 2.1 Hemispherical antenna gain pattern LEO.ANT (normalized to vertical gain 0 dB)

2.7 Postprocessing

As part of the test evaluation process, reference values for the measured GPS raw data and navigation solutions are required. These data can be extracted from the real-time log file[1] of a specific simulation using OCL command language scripts. The step size should be chosen as 1 s in accord with the sampling interval of the logged data[2] to enable the most accurate interpolation. Sample script file for extracting the LEO spacecraft ephemeris as well as simulated pseudoranges and pseudorangerates are given in Annex A.2.

2.8 Simulation Summary

A summary of the simulation scenario is given in Figs. 2.2 and 2.3 showing the elevation and signal strength for all simulated GPS satellites.

[1] The “Logging” button in the “Realtime Simulation” control screen must be checked to activate the creation of a real-time simulation log file. It desired, a log file can also be created in “Turbo Mode” (by activating the respective button in the same screen)) at about six times the natural speed. The Turbo Mode is only available, however, if the signal generation has been disabled by checking the “No hardware (dummy run)” entry in the “Options” menu of the main simulator window prior to starting a .

[2] While the simulator supports data output at sub-second intervals, any intermediate points are obtained by internal interpolation of 1 s data, which results in an associated loss of accuracy.

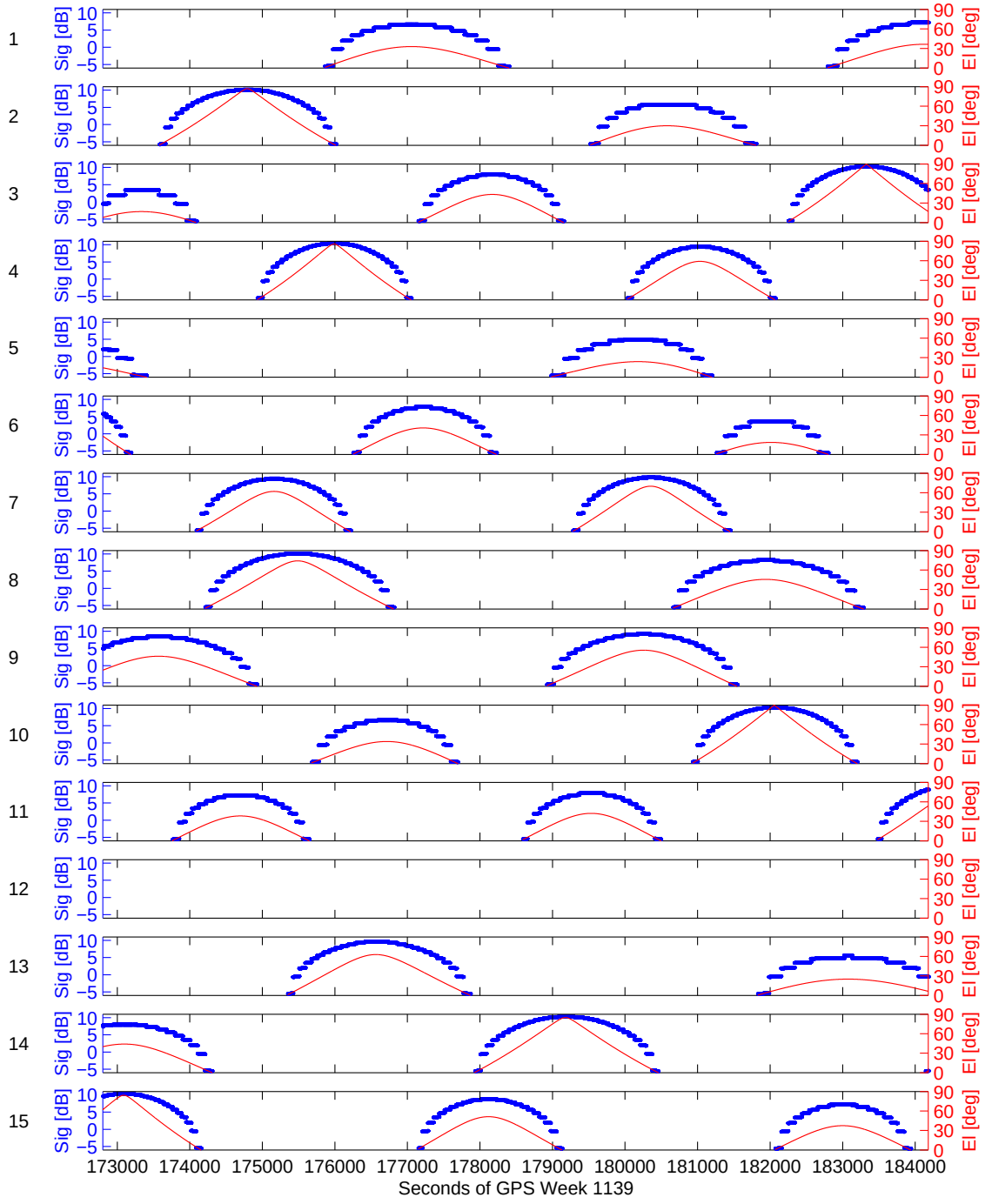

Fig 2.2 Signal strength and elevation for simulated GPS satellites in LEO scenario (PRN1-15)

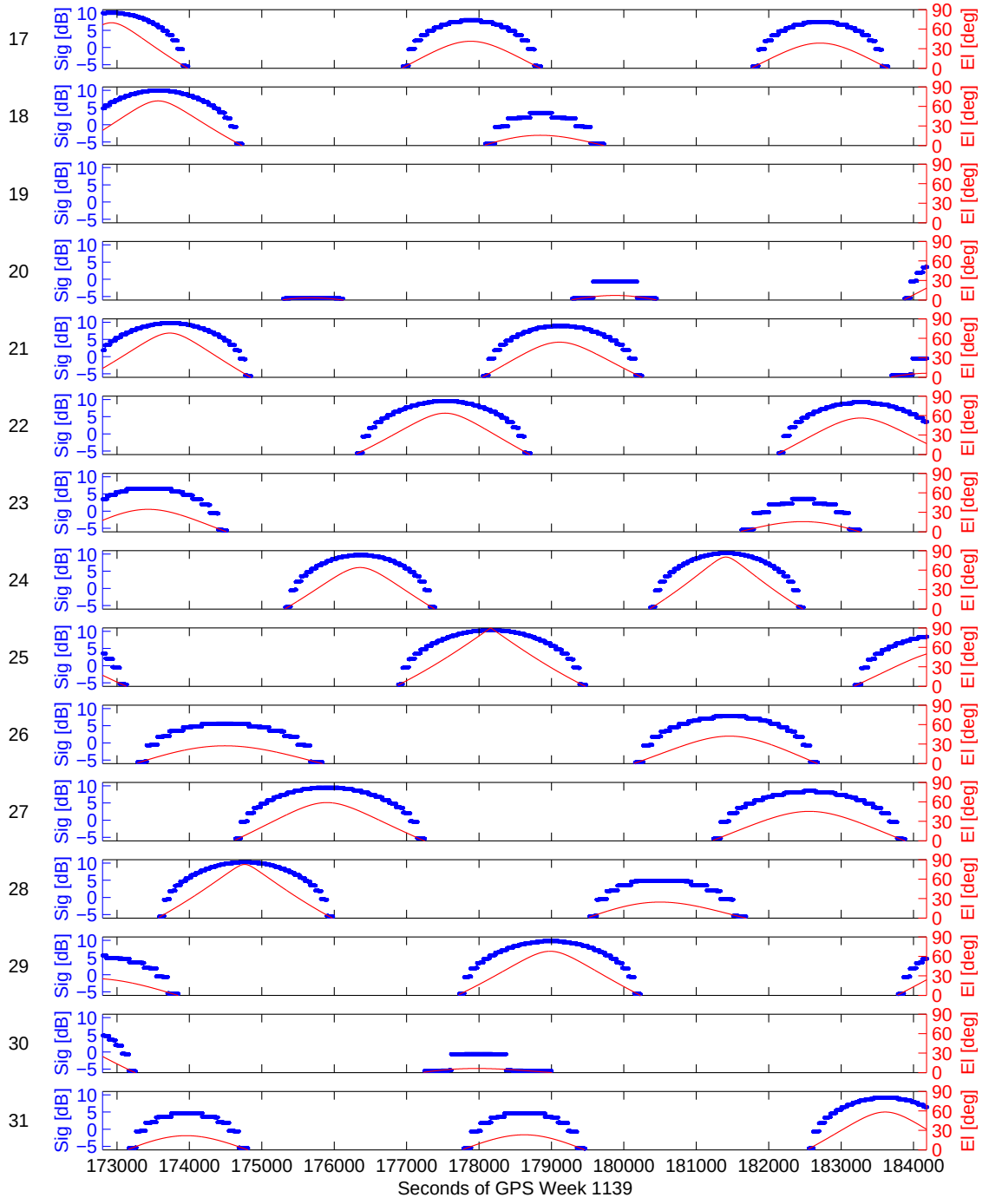

Fig 2.3 Signal strength and elevation for simulated GPS satellites in LEO scenario (PRN 17-31)

3. Test Description

3.1 Test Tree

An overview of all tests required for the performance assessment of a single frequency spaceborne GPS receiver is given in Table 3.1.

Table 3.1 Summary of test cases

Test	Scope	Configuration
A	Characterization of navigation performance • RTN position accuracy (noise level, smoothing) • RTN velocity accuracy (noise level; phase/Doppler based)	LEO_NOERR scenario normal signal level 2^h duration
B	Characterization of clock performance • Clock error (magnitude, variation, noise level) • Frequency error (magnitude, variation, noise level)	Same as A
C	Characterization of navigation performance in presence of ephemeris and ionospheric errors • Response to constellation changes and code/carrier divergence (implications of smoothing)	LEO_EPHION scenario normal signal level 2^h duration
D	Assessment of raw data quality • C/A code pseudorange (noise, systematic errors, smoothing) • L1 carrier phase (noise, systematic errors, cycle slips) • Doppler (noise)	Same as A

In case of limited test time, priority should be given to the execution of tests A and D, which provide the key accuracy figures for a receiver performance assessment. The tests are designed to require only one common simulator run, if all relevant navigation data and raw data are recorded jointly.

To identify a signal level dependence of the tracking performance, it is recommended to conduct Tests A and D with different signal power settings (nominal, +3dB, -3dB).

The tests shall, furthermore, be complemented by a summary of the receiver architecture and specific features (tracking loops, measurement sampling, timing concept, etc.) as known from independent sources.

3.2 Test A – Navigation Performance

Scope

The purpose of this test consists in the characterization of the navigation solution and the quantitative assessment of its accuracy in the absence of intentional error sources.

Test Procedure

#	Step	Remarks
1	**Execute simulation**	
1.1	Start scenario LEO_NOERR	
1.2	Perform warm (or cold) start of GPS receiver and configure desired operations parameters	
1.3	Adjust signal power setting of the simulator to obtain SNR values matching those of terrestrial open air tests. If necessary, repeat from Step 1.1.	May be skipped, if proper signal power setting is known from previous tests. Use plot of SNR versus range for best calibration results.
1.4	Record - navigation solution (time, position, velocity) - estimated clock-offset (if applicable) - number of tracked satellites (**TBC**) for 2 hours	In parallel, the following data may be recorded for use in other tests: - estimated oscillator error - signal-to-noise-ratio - raw measurements
2	**Postprocessing**	
2.1	Convert native receiver output to tabular ASCII file containing - GPS time (week, secs) - Cartesian WGS84 position vector [m] - Cartesian WGS84 velocity vector [m] - Number of tracked satellites (**TBC**) Store result in LEO_A_<rcv-id>.txt	If necessary, obtain GPS time of navigation solution from receiver clock and clock offset.
2.2	Extract simulated spacecraft trajectory at 1s stepsize into LEO_NoErr_ECEF.csv.	Optionally, convert reference trajectory to SP3 format and store in LEO_NoErr.sp3.
3	**Test Evaluation**	
3.1	Compute differences of receiver navigation solution and reference trajectory. Interpolate reference trajectory, if receiver data are collected at non-integer seconds.	A 3rd order Hermite polynomial based on position and velocity at subsequent 1s steps allows interpolation to ca. 1 mm and xxx mm/s (**TBC**)
3.2	Project errors on radial, along-track, and cross-track units vectors (RTN) as computed from the reference trajectory	
3.3	Plot RTN position and velocity errors versus GPS time over the simulation arc ([172800s, 180000s])	
3.4	Compute mean value and standard deviation (rms) of total position/velocity error and RTN components	
3.5	Interpret test results and relate the obtained performance to the receiver architecture	- Use of smoothed or raw pseudoranges? - Use of range rate from Doppler or carrier phase?

To identify a signal level dependence of the tracking performance, it is recommended to conduct Test A repeatedly with varied signal power settings (e.g. nominal, +3dB, -3dB).

3.3 Test B – Clock Performance

Scope

The purpose of this test consists in the characterization of the navigation solution and the quantitative assessment of its accuracy in the absence of intentional error sources.

Test Procedure

#	Step	Remarks
1	**Execute simulation**	May be skipped if applicable data have already been recorded as part of Test A
1.1	Start scenario LEO_NOERR and set signal power in accord with results of Test 1A, Step 1.2	
1.2	Perform warm (or cold) start of GPS receiver and configure desired operations parameters	
1.3	Record - raw measurements for 2 hours	
2	**Postprocessing**	
2.1	Convert the available raw measurements (pseudo-range, carrier phase, Doppler) into RINEX observation format. Store result in LEO_B_<rcv-id>.rnx	Time tags in receiver time
2.2	Extract simulated pseuodranges and pseudorange-rates at 1s stepsize into LEO_NoErr_PR.csv and LEO_NoErr_PRR.csv	May be replaced by off-line computation of pseudorange and pseudorange-rate from the simulated spacecraft ephemeris
3	**Test Evaluation**	
3.1	- Compute receiver clock offset (in [ns]) from single point position solution using observed and modeled pseudoranges for each observation epoch. - Plot clock error versus GPS time over the simulation arc ([172800s, 180000s])	A 3rd order Hermite polynomial based on pseudorange and pseudorange-rate at subsequent 1s steps allows adequate interpolation (**TBC**) of both values if receiver data are collected at non-integer seconds.
3.2	- Compute receiver clock frequency error (in [Hz]) from single point velocity solution using Doppler based and modeled pseudorange-rates for each observation epoch. - Plot clock drift versus GPS time over the simulation arc ([172800s, 180000s])	
3.3	- Compute receiver clock frequency error (in [Hz]) from single point velocity solution using carrier phase based and modeled pseudorange-rates for each observation epoch. - Plot clock drift versus GPS time over the simulation arc ([172800s, 180000s])	The range-rate can be obtained from a quadratic fit of three consecutive carrier phase readings.
3.4	Interpret test results and relate the obtained performance to the receiver architecture	- Is the clock error confined to a certain deadband or growing beyond bounds? - Does the receiver clock control involve any filtering or smoothing? - Are Doppler and carrier phase measurements based on the same clock as the pseudorange measurements?

3.4 Test C – Navigation Performance with Ephemeris and Ionosphere Errors

Scope

The purpose of this test consists in the characterization of the navigation solution in the presence of intentional broadcast ephemeris errors as well as ionospheric refraction.

Test Procedure

#	Step	Remarks
1	**Execute simulation**	
1.1	Start scenario LEO_EPHION and set signal power in accord with results of Test A, Step 1.2	
1.2	Perform warm (or cold) start of GPS receiver and configure desired operations parameters	
1.4	Record - navigation solution (time, position, velocity) - estimated clock-offset (if applicable) - number of tracked satellites (**TBC**) for 2 hours	
2	**Postprocessing**	
2.1	Convert native receiver output to tabular ASCII file containing - GPS time (week, secs) - Cartesian WGS84 position vector [m] - Cartesian WGS84 velocity vector [m] - Number of tracked satellites (**TBC**) Store result in LEO_C_<rcv-id>.txt	If necessary, obtain GPS time of navigation solution from receiver clock and clock offset.
2.2	Extract simulated spacecraft trajectory at 1s stepsize into LEO_EphErr_ECEF.csv. Optionally, convert to SP3 format and store in LEO_EphErr.sp3.	
3	**Test Evaluation**	
3.1	Compute differences of receiver navigation solution and reference trajectory. Interpolate reference trajectory, if receiver data are collected at non-integer seconds.	A 3rd order Hermite polynomial based on position and velocity at subsequent 1s steps allows interpolation to ca. 1 mm and xxx mm/s (**TBC**)
3.2	Project errors on radial, along-track, and cross-track units vectors (RTN) as computed from the reference trajectory	
3.3	Plot RTN position and velocity errors versus GPS time over the simulation arc ([172800s, 180000s])	
3.4	Compute mean value and standard deviation (rms) of total position/velocity error and RTN components	
3.5	Interpret test results and relate the obtained performance to the receiver architecture	- Response to changes in the set of tracked satellites (immediate or delayed)? - Amplitude and time scale of code-carrier divergence? - Application of ionospheric refraction correction (from amplitude of mean radial position offset)?

To identify a signal level dependence of the tracking performance, it is recommended to conduct Test D repeatedly with varied signal power settings (e.g. nominal, +3dB, -3dB).

3.5 Test D – Raw Measurements Accuracy

Scope

The purpose of this test consists in a quantitative accuracy assessment of the raw measurements (pseudorange, carrier phase, Doppler) and the identification of systematic tracking errors.

Test Procedure

#	Step	Remarks
1	**Execute simulation**	May be skipped if applicable data have already been recorded as part of Test A
1.1	Start scenario LEO_NOERR and set signal power in accord with results of Test A, Step 1.2	
1.2	Perform warm (or cold) start of GPS receiver and configure desired operations parameters	
1.3	Record - raw measurements for 2 hours	
2	**Postprocessing**	
2.1	Convert measurement time tags from receiver time to GPS time using receiver internal clock solution or offline clock offset determination (cf. Test B, Step 3.1)	Obsolete, if Test B indicates clock errors of less than 0.1 μs (30 m)
2.2	- Convert the available raw measurements (pseudorange, carrier phase, Doppler) into RINEX observation format. - Store result in LEO_D_<rcv-id>.rnx	Using best available clock solution for GPS time tags
2.3	Extract simulated pseuodranges and pseudorange-rates at 1s stepsize into LEO_NoErr_PR.csv and LEO_NoErr_PRR.csv	May be replaced by off-line computation of pseudorange and pseudorange-rate from the simulated spacecraft ephemeris
3	**Test Evaluation**	
3.1	- Obtain double differences (i.e. inter-channel difference of observed-modelled data) of raw pseudorange, carrier phase and Doppler measurements for PRN# 2-28 during t=[174000 s, 175800 s] and PRN# 14-29 during t=[178000 s, 180100 s] and PRN# 3-15 during t=[177100 s, 179100 s] - Normalize initial carrier phase DD to zero. - Plot results and compute standard deviations (rms) for undifferenced data (=$\sigma(\mathrm{DD})/\sqrt{2}$)	Common dynamics cancels loop errors
3.2	Same for PRN# 21-28 during t=[173900 s, 174700 s] and PRN# 13-22 during t=[176400 s, 177700 s] and PRN# 6-17 during t=[177100 s, 178100 s]	Line of sight acceleration varies by ±1g; allows identification of steady state error in low order tracking loops
3.4	Interpret test results and relate the obtained performance to the receiver architecture	- Do the measurements exhibit timing errors? - Do the measurements exhibit an acceleration dependence (2^{nd} order tracking loop limitation)?

Notes

After collecting the raw measurements over a two hour data arc, modeled pseudoranges and range rates are computed based on the simulated spacecraft trajectory and the known GPS constellation almanac. These are subtracted from the measurements to remove the varying geometry between the receiver and the GPS satellites from the data (cf. Fig. 3.1). The result is essentially the sum of receiver clock errors (δt, δf), as well as measurement noise and tracking loop related errors (ε_i). To further eliminate the dominating clock terms, differences

of two channels (A & B) are subsequently formed. Ideally, this results in a zero mean, white noise sequence with a variance equal to the sum of the noise variance of the individual channels. For two channels with similar signal-to-noise (SNR) ratios, the noise errors are expected to be of equal size and the r.m.s noise of the inter-channel difference is just $\sqrt{2}$ times as large as that of the undifferenced measurements.

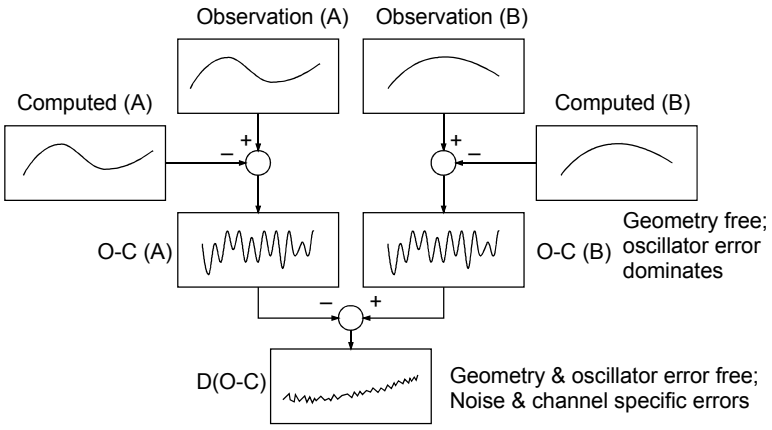

Fig. 3.1 Data analysis concept for assessment of raw data quality from measured and simulated pseudorange, carrier phase or Doppler data

Suitable time intervals and GPS satellite combinations offering either common or widely different signal dynamics are collated in Table 3.2. Depending on the initialization time of the GPS receiver some of the early time intervals may not be accessible in a particular test.

Table 3.2 Recommended double difference combinations (A-B) for analysis of raw data quality

#	PRN A	PRN B	Start	End	Description
1	2	28	174000 s	175800 s	low relative dynamics ([-0.5,0.0] km/s, ±0.05g), high signal level
2	14	29	178100 s	180000 s	low relative dynamics ([-2,0] km/s, ±0.2), high signal level
3	3	15	177400 s	178900 s	low relative dynamics (±1 km/s, ±0.2g), medium high signal level
4	21	28	173800 s	174700 s	high relative dynamics ([8,10] km/s, ±1g), high signal level
5	13	22	176500 s	177700 s	high relative dynamics ([3,8] km/s, ±1g), high signal level
6	6	17	177100 s	178000 s	high relative dynamics ([4,7] km/s, ±0.8g), medium signal level

4. GPS Orion Receiver Test

4.1 Receiver Description

The GPS Orion receiver represents a prototype design [5] of a terrestrial GPS receiver built around the Mitel (now Zarlink) GP2000 chipset. It comprises a GP2015 R/F front end and DW9255 saw filter, a GP2021 correlator as well as an ARM60B 32-bit microprocessor. The receiver provides C/A code tracking on 12 channels at the L1 frequency and operates with an active antenna having a total gain of roughly 28 dB. It offers a battery backed real-time clock and non-volatile memory to maintain relevant data while disconnected from the main power supply. For use on low Earth satellites and other space applications numerous modifications and enhancements have been made to the original firmware by DLR. These include e.g.

- corrections to the Doppler prediction, measurement time tagging and navigation algorithms to allow proper tracking and navigation at high velocities,
- the synchronization of all measurements with integer GPS seconds,
- the aiding of the acquisition process using a priori trajectory information to facilitate a receiver hot (or warm) start,
- the provision of carrier phase measurements based on a 3rd order PLL with FLL assist,
- the computation of carrier phase smoothed pseudoranges and carrier based range-rate,
- a kinematic relative positioning using two receivers,
- as well as an improved telemetry and telecommand interface.

In total, the Orion receiver provides five different kinds of raw and preprocessed measurements. Smoothed pseuderange and range-rate are given in the F41 message while the unmodified pseudorange, Doppler based range rate and carrier phase measurements are available as part of the F42 message. The carrier smoothing of raw pseudoranges employs a typical filtering time scale of 25 s, which is shorter than that applied in many terrestrial receivers but reduces the impact of code-carrier divergence in space applications with rapidly varying elevation angles. Smooth range rates are derived internally from three consecutive 0.1s carrier phase samples, thus yielding uncorrelated range rates at the 1 Hz output interval

The navigation solution is computed once per second using carrier phase smoothed pseudoranges and carrier derived range-rate measurements. No ionospheric (or tropospheric) corrections are applied in orbit mode.

The primary time and frequency source of the receiver consist of temperature controlled oscillator (TCXO) with a nominal frequency of 10 MHz and a specified tolerance of 2 ppm. The receiver employs a linear clock model to relate oscillator based clock tics to GPS time. Updates of the clock model parameters are computed once per second as part of the navigation solution if the receiver is tracking at least four satellites. The modeled GPS times provides the reference for the collection of pseudorange measurements inside the receiver and for time tagging the various raw measurements. In an S/A free environment, the modeled GPS time typically agrees with the true GPS time to within 30 m or 100 ns. Carrier phase measurements are likewise referred to the modeled GPS time clock to allow a direct comparison with pseudoranges and their use for carrier phase smoothing. The (pseudo-)range-rate measurements in contrast, exhibit a common bias on all channels that matches the instantaneous error of the reference oscillator.

4.2 Test Configuration

A summary of the employed test hardware and software is given in Table 4.1. All tests were conducted at the Center for Space Research, The University of Texas at Austin.

Table 4.1 Hard- and software configuration used in the Orion receiver tests

Item	Description
GPS Orion receiver	DLR/GSOC board #9; Rakon IT225B oscillator S/W version DLR61707I (2002/04/28)
Preamplifier	VAS/Motorola unit #1002, 27.5dB amplification
Signal simulator	Spirent STR4760 unit #2115 (UT/CSR); 16 channels L1 (C/A + Pseudo-Y) & L2 (Pseudo-Y) Default signal power setting +8dB

4.3 Navigation Accuracy

A summary of the achieved navigation accuracy in the absence of intentional ephemeris errors or ionospheric delays (Test A) is given in Table 4.2 and Fig. 4.1. The positioning errors are generally well below 1 m and exhibit an even smaller short term noise level (<10 cm) due to the application of carrier phase smoothing (with a typical averaging time scale of 25 s). The velocity solution is accurate to better than 5 cm/s in accord with the use of carrier based range-rate measurements and an accurate range-rate modeling within the receiver. A degraded positioning accuracy may be noticed at a higher than average signal level, which is related to an increased number of outliers at the acquisition of new GPS satellites. Otherwise, the receiver shows essentially the same navigation performance over the considered range of signal levels.

Table 4.1 GPS Orion/ DLR61707I navigation solution accuracy in the absence of ephemeris and ionospheric errors (Test A)

Signal level	**Radial**	**Along-track**	**Cross-track**	**Position**
Nominal	+0.13 ± 0.39 m	–0.06 ± 0.13 m	–0.02 ± 0.10 m	+0.37 ± 0.26 m
High (+3dB)	–0.00 ± 0.64 m	+0.01 ± 0.75 m	–0.00 ± 0.18 m	+0.24 ± 0.97 m
Low (-3dB)	+0.15 ± 0.54 m	–0.17 ± 0.19 m	–0.02 ± 0.10 m	+0.51 ± 0.38 m
Signal level	**Radial**	**Along-track**	**Cross-track**	**Velocity**
Nominal	+0.00 ± 0.03 m/s	0.00 ± 0.01 m/s	-0.00 ± 0.01 m/s	+0.03 ± 0.02 m/s
High (+3dB)	+0.00 ± 0.03 m/s	0.00 ± 0.01 m/s	-0.00 ± 0.01 m/s	+0.03 ± 0.02 m/s
Low (-3dB)	+0.00 ± 0.04 m/s	0.00 ± 0.02 m/s	-0.00 ± 0.01 m/s	+0.04 ± 0.02 m/s

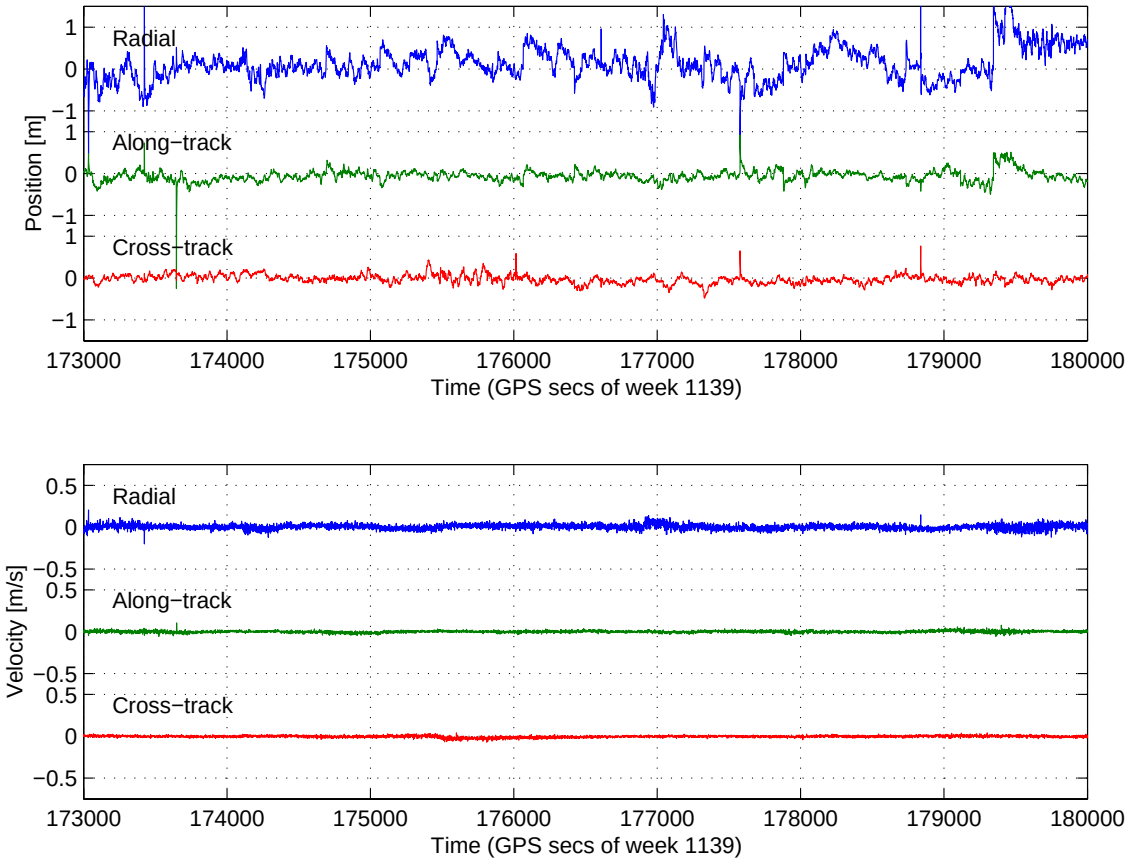

Fig. 4.1 GPS Orion/DLR61707I navigation accuracy in the absence of ephemeris and ionospheric errors

4.4 Clock Characteristics

The clock characteristics of the GPS Orion receiver are illustrated by the results of Test B shown in Fig. 4.2. As mentioned in Sect. 4.1, the measurement time tags as well as the pseudorange values are referred to a GPS time model clock maintained by the receiver. Therefore, the pseudorange measurements[3] are essentially bias free and the offline determination of the receiver clock bias from carrier smoothed pseudoranges exhibits a zero-mean error with a standard deviation of only 1.5 ns (45 cm). The range-rate measurements, in contrast, are referred to the free-running oscillator[4] and thus exhibit a common bias that corresponds to the oscillator frequency offset at the measurement epoch. Aside from a long term frequency drift, the employed oscillator exhibits a short term noise of about 3 Hz (equivalent to 0.6 m/s), which is illustrated in Fig. 4.2 (bottom).

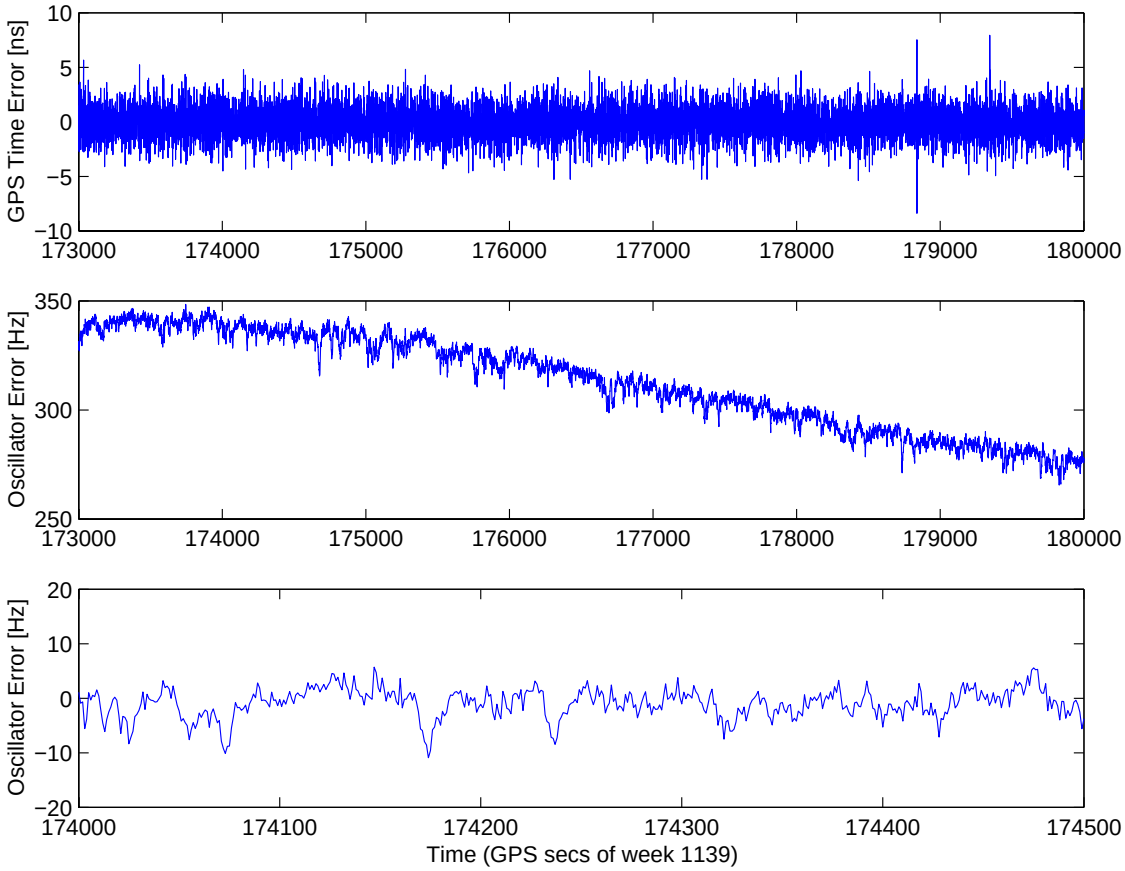

Fig. 4.2 GPS Orion model clock error (top) and oscillator frequency stability (center, bottom) as derived from the common bias of smoothed pseudorange measurements as well as *internally* computed carrier based range-rate measurements (Test B)

[3] The carrier phase measurements output as part of the F42 message are likewise referred to the modeled GPS clock and the change in carrier phase is such an unbiased measure of the range variation.
[4] For consistency between the F42 and F41 message generated by the Orion receiver, both the Doppler based range-rate and the internally computed carrier based range rate exhibit the same oscillator related bias.

4.5 Navigation Accuracy with Ephemeris and Ionosphere Errors

A summary of the achieved navigation accuracy in the presence of intentional ephemeris errors and ionospheric delays (Test C) is given in Table 4.3 and Fig. 4.3. As expected, the position solution exhibits pronounced steps when new satellites are acquired. A large scatter is obvious in all components of the position vector and the radial component exhibits a mean offset of about 12 m resulting from the elevation dependent ionospheric path delay. The horizontal plane coordinates, in contrast are essentially unbiased. Despite the large overall errors, the position solutions exhibits a very small short term noise due to the application of carrier phase smoothing. The velocity solution exhibits no changes compared to the error free scenario discussed above, since the modeling of broadcast ephemeris errors in the Spirent signal simulator does not allow the incorporation of dedicated velocity terms. Both position and velocity are degraded during the first 500 s of the test run when the receiver did not properly acquire all visible satellites. As result of the reduced PDOP the noise and systematic errors of the navigation solution are more pronounced during this time interval than for the subsequent data arc.

Table 4.3 GPS Orion navigation solution accuracy in the presence of ephemeris and ionospheric errors (Test C)

Signal level	**Radial**	**Along-track**	**Cross-track**	**Position**
Nominal	+15.0 ± 14.6 m	–2.4 ± 6.6 m	+1.8 ± 2.8 m	+16.9 ± 14.6 m
Signal level	**Radial**	**Along-track**	**Cross-track**	**Velocity**
Nominal	+0.01 ± 0.04 m/s	–0.02 ± 0.02 m/s	–0.00 ± 0.01 m/s	+0.04 ± 0.03 m/s

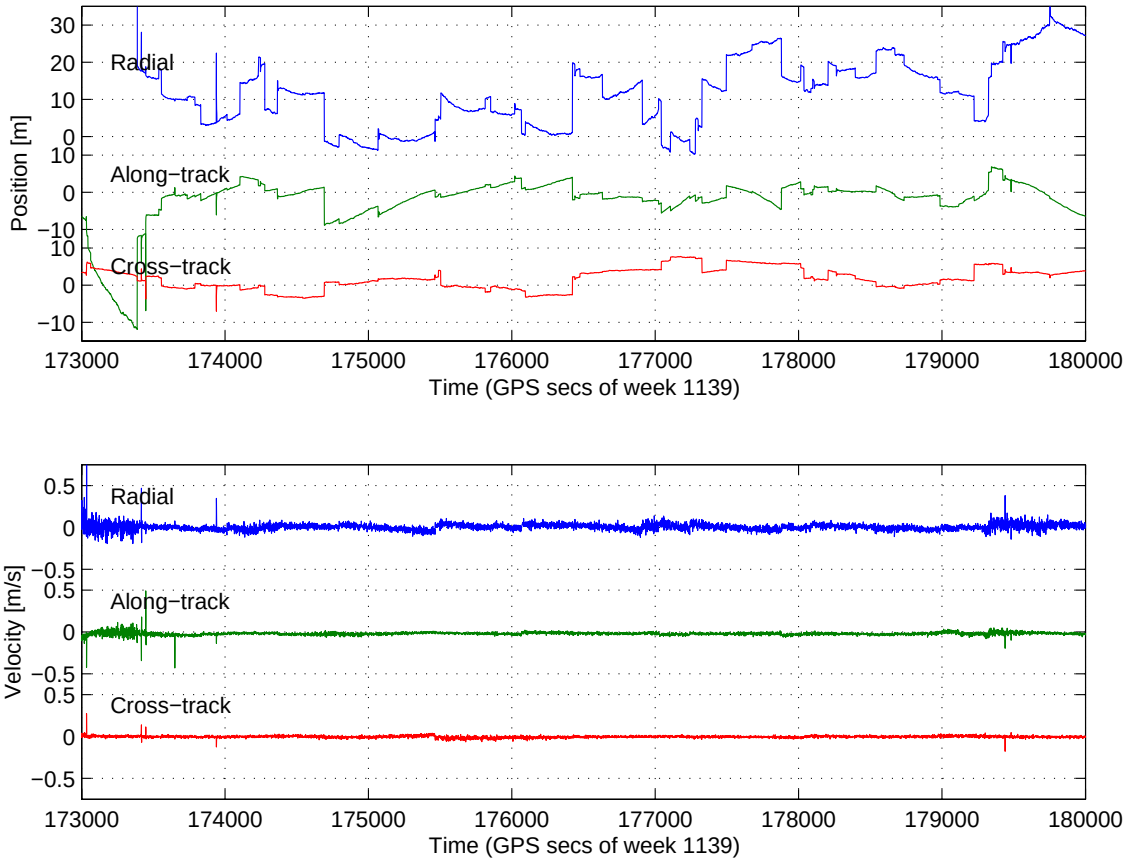

Fig. 4.3 GPS Orion/DLR61707I navigation accuracy in the presence of ephemeris and ionospheric errors

4.6 Raw Measurements Accuracy

Results of Test D for the assessment of the raw data quality are collated in Table 4.4. The resulting pseudoranges are typically accurate to 1 m, carrier phase measurements have r.m.s. errors of 0.5-0.8 mm and the Doppler base range-rate is accurate to about 8 cm/s. The carrier phase smoothed pseudoranges exhibit a noise level of typically 0.15 m, while carrier based range rates are accurate to 1 cm/s. The latter value is consistent with the observed carrier phase noise and the differencing over adjacent 0.1 s samples.

Aside from the default signal level, the various test cases have been executed for both a 3 dB increase and decrease of the simulator output power settings. As expected, the quality of the carrier phase and Doppler measurements varies with the applied signal level and resulting signal-to-noise ratio. On average the noise level changes by 20% for a 3 dB SNR variation in accord with theoretical predictions. The pseudorange accuracy, in contrast, is essentially constant over the tested signal level range within an overall scatter of about 5%. For further reference, the relation between measurement noise and signal-to-noise ratio (SNR) readings of the Orion receiver is illustrated in Fig. 4.4 for carrier phase and Doppler measurements. The specified SNR values refer to the center time of test cases 1–6, and are about 3 dB higher than the average SNR over the respective time intervals.

Sample plots of double differences between individual channels are shown in Figs. 4.5 and 4.6 for nominal signal levels. While case 1 (PRN 2-28, cf. Fig. 4.5) illustrates a situation in which the signals from both satellites are affected by an almost identical dynamics, maximum relative accelerations of ±1g and range rate differences of up to 10 km/s are encountered in case 4 (PRN 2-28, Fig. 4.6). None of the available data types exhibits evidence of systematic errors related to the range rate or line of sight acceleration, thus confirming the proper function of the tracking loops and the accurate time tagging of all measurements.

Table 4.4 Standard deviation of GPS Orion raw data obtained from Test D (C1=pseudorange, L1=carrier phase, D1= range rate from Doppler, C1(CP)=carrier smoothed pseudorange, D1(CP)=range rate from carrier phase)

Signal level	#	PRN	Interval	C1	L1	D1	C1(CP)	D1(CP)
Normal	1	2–28	[174000s,175800s]	0.93 m	0.46 mm	0.06 m/s	0.09 m	0.01 m/s
	2	14–29	[178100s,180000s]	0.91 m	0.50 mm	0.07 m/s	0.17 m	0.01 m/s
	3	3–15	[177400s,178900s]	0.91 m	0.63 mm	0.08 m/s	0.13 m	0.01 m/s
	4	21–28	[173800s,174700s]	0.94 m	0.76 mm	0.08 m/s	0.10 m	0.01 m/s
	5	13–22	[176500s,177700s]	0.90 m	0.68 mm	0.08 m/s	0.12 m	0.01 m/s
	6	6–17	[177100s,178000s]	0.94 m	0.69 mm	0.08 m/s	0.13 m	0.02 m/s
High (+3dB)	1	2–28	[174000s,175800s]	0.96 m	0.38 mm	0.05 m/s	n.a.	n.a.
	2	14–29	[178100s,180000s]	1.02 m	0.41 mm	0.05 m/s	n.a.	n.a.
	3	3–15	[177400s,178900s]	0.94 m	0.53 mm	0.06 m/s	n.a.	n.a.
	4	21–28	[173800s,174700s]	0.97 m	0.66 mm	0.06 m/s	n.a.	n.a.
	5	13–22	[176500s,177700s]	0.93 m	0.61 mm	0.06 m/s	n.a.	n.a.
	6	6–17	[177100s,178000s]	0.93 m	0.60 mm	0.07 m/s	n.a.	n.a.
Low (-3dB)	1	2–28	[174000s,175800s]	0.94 m	0.63 mm	0.09 m/s	0.15 m	0.01 m/s
	2	14–29	[178100s,180000s]	0.92 m	0.65 mm	0.09 m/s	0.17 m	0.02 m/s
	3	3–15	[177400s,178900s]	0.94 m	0.79 mm	0.11 m/s	0.14 m	0.02 m/s
	4	21–28	[173800s,174700s]	0.94 m	0.84 mm	0.10 m/s	0.15 m	0.02 m/s
	5	13–22	[176500s,177700s]	0.96 m	0.83 mm	0.10 m/s	0.15 m	0.02 m/s
	6	6–17	[177100s,178000s]	0.95 m	0.85 mm	0.11 m/s	0.18 m	0.02 m/s

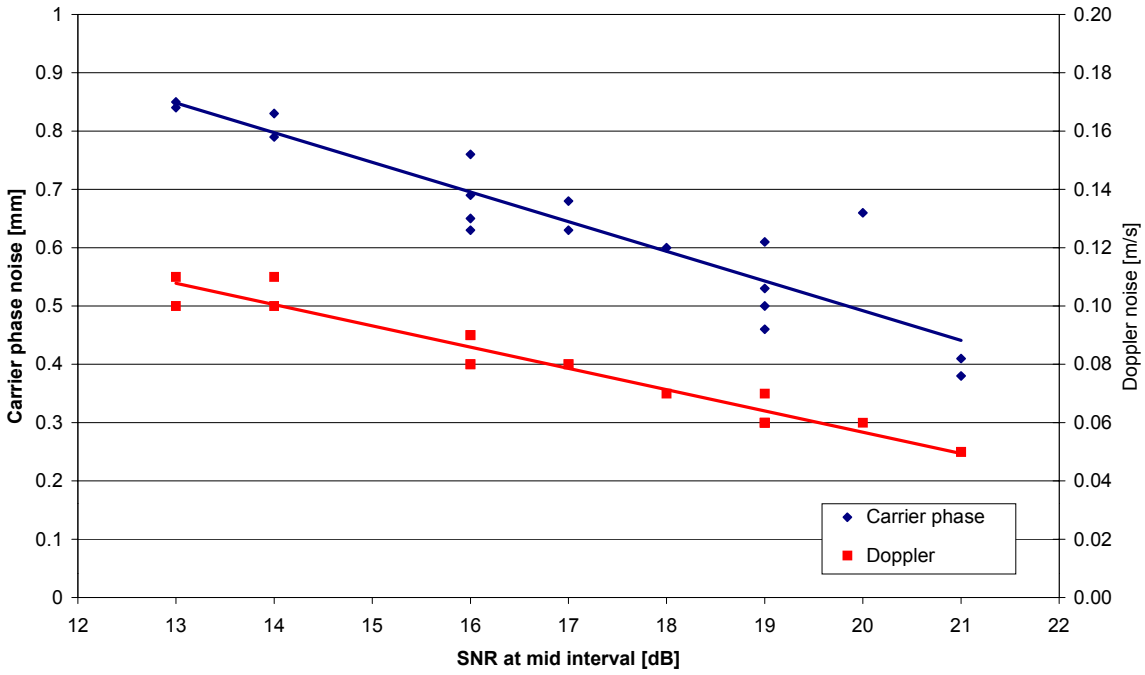

Fig. 4.4 Average carrier phase and Doppler noise as a function of signal-to-noise ratio (SNR) near center of data arc.

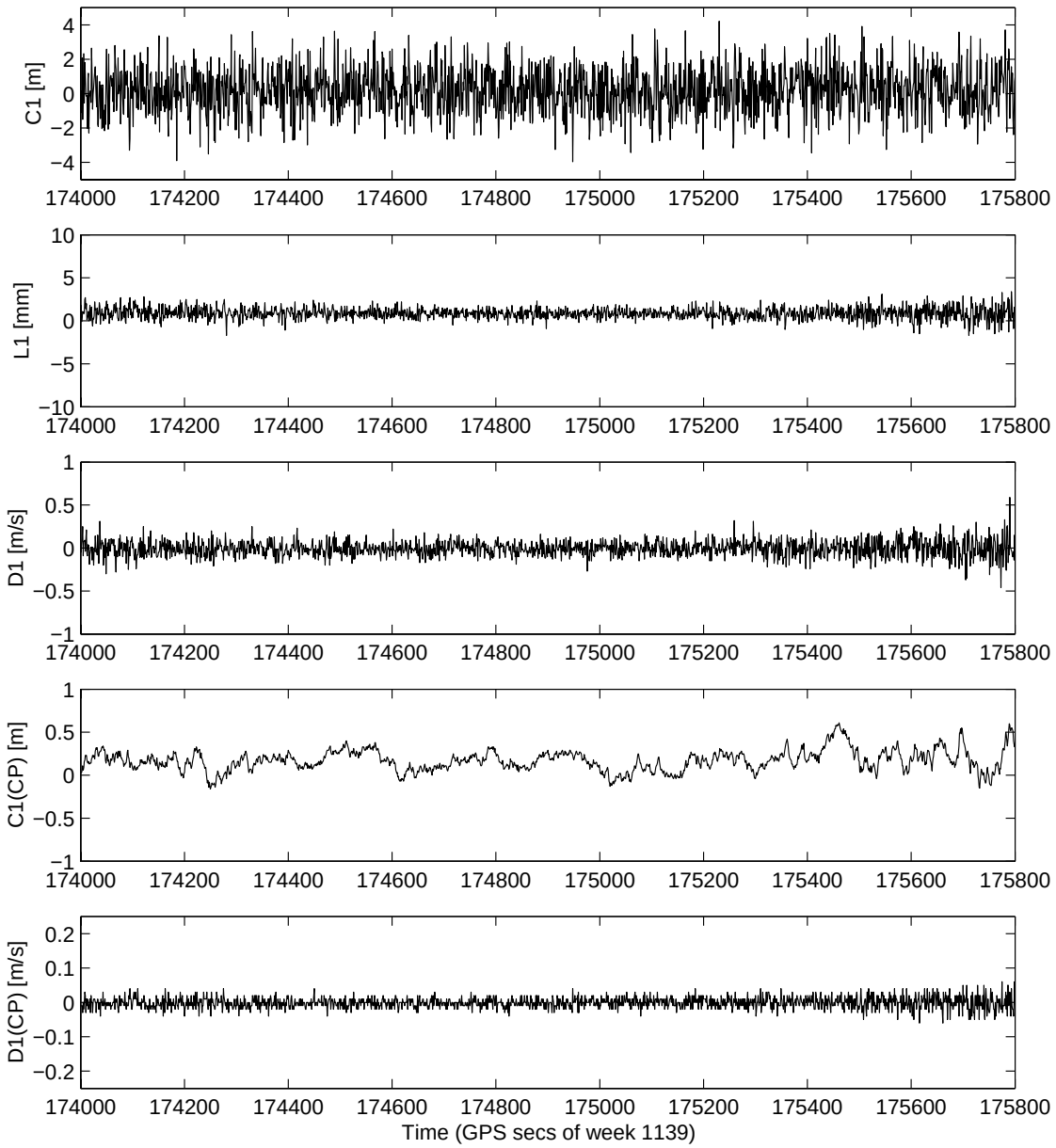

Fig. 4.5 Double differences (PRN 2-28, observed-modeled) of GPS Orion measurements obtained in Test D1 (low relative dynamics) at nominal signal level (C1=pseudorange, L1=carrier phase, D1= range rate from Doppler, C1(CP)=carrier smoothed pseudorange, D1(CP)=range rate from carrier phase)

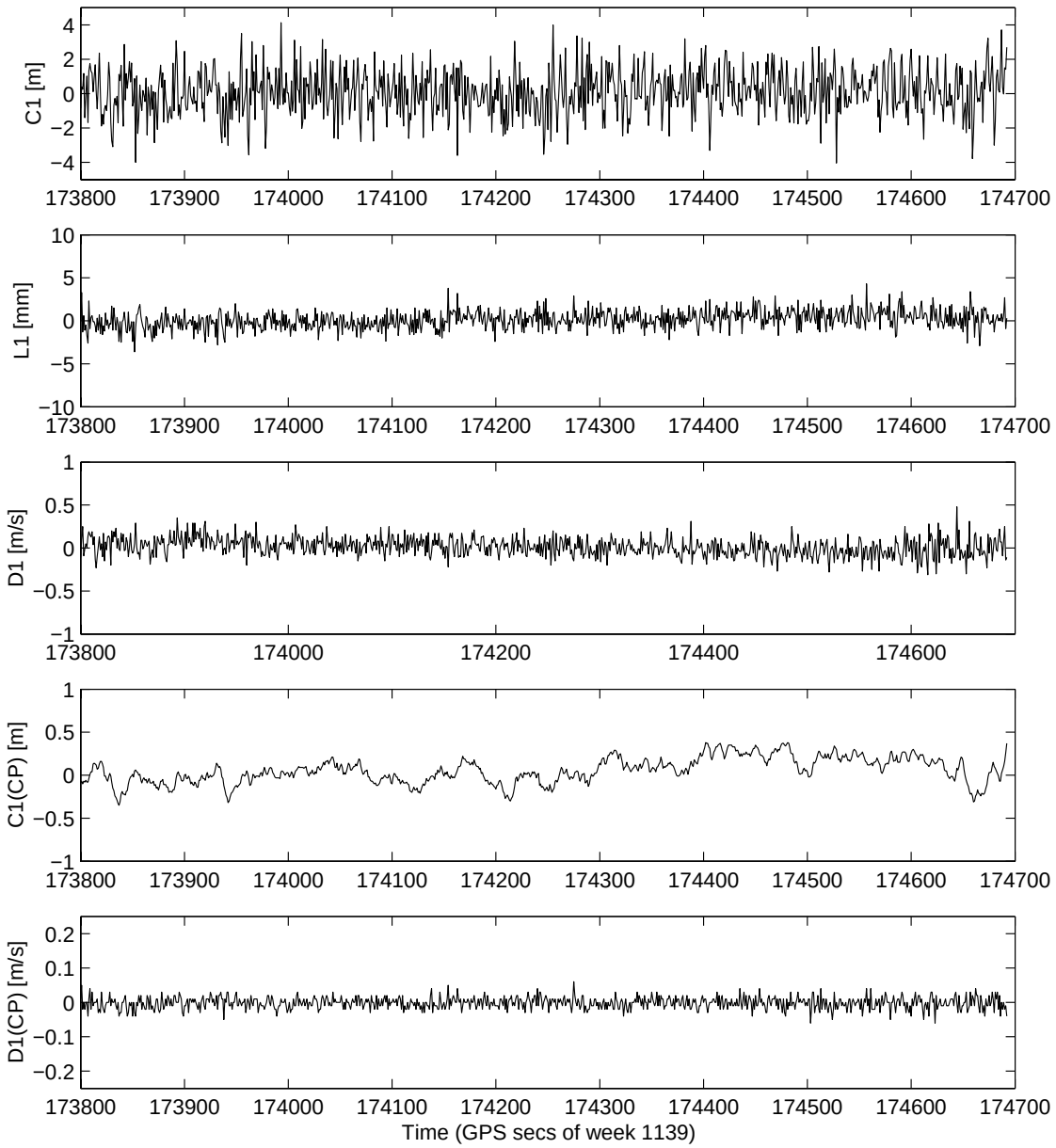

Fig. 4.6 Double differences (PRN 21-28, observed-modeled) of GPS Orion measurements obtained in Test D4 (high relative dynamics) at nominal signal level (C1=pseudorange, L1=carrier phase, D1= range rate from Doppler, C1(CP)=carrier smoothed pseudorange, D1(CP)=range rate from carrier phase)

4.7 Comparison with GPS Architect

The GPS Architect receiver is essentially hard- and software compatible to the Orion receiver but offers a dedicated serial interface for software downloads from a host PC as well as debugging purposes. Despite the apparent similarity, it has previously been noted (cf. [6]) that the reference frequency of the Orion receiver is generally less stable than that of the Architect receiver. Since the employed temperature controlled oscillators have similar characteristics and specifications, it is most likely that the degraded performance is due to a tighter integration and the lack of a separate front end power supply in the GPS Orion board.

Comparison tests conducted with s/w version DLR6170I confirm the different clock behavior but show an essentially identical tracking performance for both platforms. The standard deviation of the GPS Architect[5] clock error determined in Test B amounts to 0.3 ns (ca. 10 cm), which is five times better than for the Orion receiver. Likewise the frequency noise of 0.25 Hz (equivalent to 5 cm/s) is found to be better by a factor of ten (Fig. 4.7).

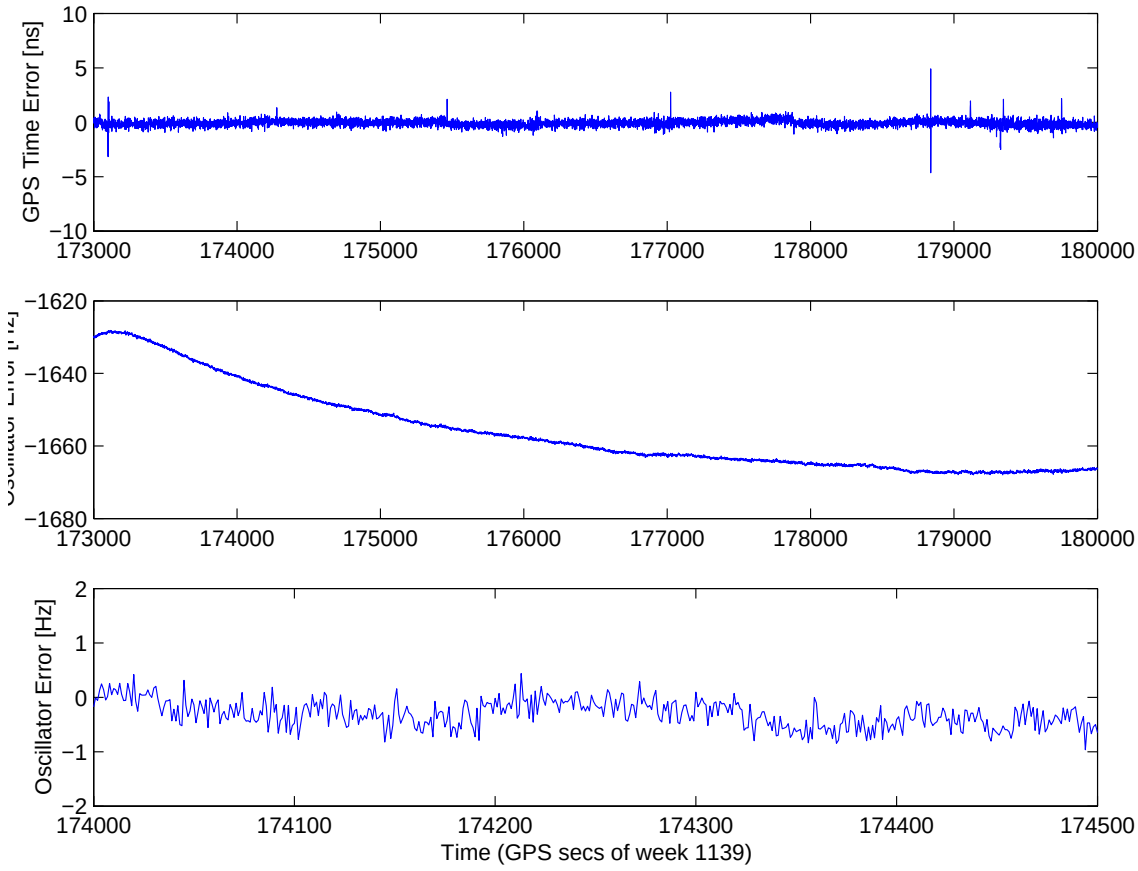

Fig. 4.7 GPS Architect model clock error (top) and oscillator frequency stability (center, bottom) as derived from the common bias of smoothed pseudorange measurements as well as *internally* computed carrier based range-rate measurements (Test B)

Despite the notably different clock characteristics, the GPS Orion and GPS Architect receivers exhibited almost identical noise values for the raw pseudorange, carrier phase and Doppler measurements for the employed s/w version DLR6170I. This is in contrast to s/w version DLR61707H (using a wide band 2nd order PLL with FLL assist for carrier tracking), which showed a degraded performance of the Orion board at low SNR values.

[5] The tests were conducted using the GPS Architect receiver of UT/CSR (serial no. 133).

4.8 Summary

The signal simulator tests of a GPS Orion unit running s/w version DL61707I demonstrates a proper function and accurate tracking of the receiver. Noise values of 1 m, 0.5 mm and 0.08 m/s second have been obtained for pseudorange, carrier phase and Doppler measurements at representative signal-to-noise ratios. No traces of systematic errors in the above data types have been identified, which confirms the absence of time tagging errors as well as steady state tracking errors of the employed 3rd order phase-lock-loop with FLL assist.

Acknowledgement

The work presented in this paper was performed during the first author's stay at the Center for Space Research, University of Texas (UT/CSR) within the visiting scientist program of the German Aerospace Establishment (DLR). The institutional and financial support received by these institutions is gratefully acknowledged.

References

[1] *STR Series Satellite Navigation Simulator System Reference Manual*; DGP00032AAC; Issue 11-00, May 2001.

[2] NATO Standard Agreement STANAG 4294, Issue 1.

[3] Van Dierendonck A. J.; *GPS Receivers*; chap. 8 in: Spilker J., Parkinson B., eds.; *Global Positioning System: Theory and Applications Vol. I*; American Institute of Aeronautics and Astronautics Inc., Washington (1995).

[4] *Accuracy of the GPS BO and the WAAS-corrected Orbit*; http://gauss.gge.unb.ca/grads/orbit/; University of New Brunswick (2001).

[5] Mitel; *GP2000 GPS Receiver Hardware Design*; AN4855; Mitel Semiconductor; Issue 1.4, February 1999.

[6] Montenbruck O.; *Assessment of Oscillator and Doppler Tracking Accuracy for the Mitel Architect/Orion Receiver*; DLR-GSOC TN 01-10; Deutsches Zentrum für Luft- und Raumfahrt, Oberpfaffenhofen (2001).

Annex

A.1 YUMA Almanac

The following listing provides the YUMA almanac for week 1138 (=1024+114). For generation of a GPS constellation file in the old STR2760 signal simulator, the string “Week(rad):” must be replaced by “TOA(rad): “ prior to loading the almanac file.

```
******** Week  114 almanac for PRN-01 ********
ID:                         01
Health:                     000
Eccentricity:               0.5073070526E-002
Time of Applicability(s):  589824.0000
Orbital Inclination(rad):   0.9662544983
Rate of Right Ascen(r/s):  -0.7691748964E-008
SQRT(A)  (m 1/2):           5153.681152
Right Ascen at Week(rad):   0.9516830290E+000
Argument of Perigee(rad):  -1.737205903
Mean Anom(rad):            -0.2096690706E+001
Af0(s):                     0.2021789551E-003
Af1(s/s):                   0.3637978807E-011
week:                        114

******** Week  114 almanac for PRN-02 ********
ID:                         02
Health:                     000
Eccentricity:               0.2198839188E-001
Time of Applicability(s):  589824.0000
Orbital Inclination(rad):   0.9331061322
Rate of Right Ascen(r/s):  -0.8000333246E-008
SQRT(A)  (m 1/2):           5151.900879
Right Ascen at Week(rad):   0.2945542718E+001
Argument of Perigee(rad):  -1.995584669
Mean Anom(rad):             0.1229570615E+001
Af0(s):                    -0.1001358032E-003
Af1(s/s):                  -0.7275957614E-011
week:                        114

******** Week  114 almanac for PRN-03 ********
ID:                         03
Health:                     000
Eccentricity:               0.2572536469E-002
Time of Applicability(s):  589824.0000
Orbital Inclination(rad):   0.9353831349
Rate of Right Ascen(r/s):  -0.8057478483E-008
SQRT(A)  (m 1/2):           5153.637207
Right Ascen at Week(rad):  -0.2259582163E+001
Argument of Perigee(rad):   0.517855585
Mean Anom(rad):            -0.1247363069E+000
Af0(s):                     0.8010864258E-004
Af1(s/s):                   0.3637978807E-011
week:                        114

******** Week  114 almanac for PRN-04 ********
ID:                         04
Health:                     000
Eccentricity:               0.5658626556E-002
Time of Applicability(s):  589824.0000
Orbital Inclination(rad):   0.9721267685
Rate of Right Ascen(r/s):  -0.8194627053E-008
SQRT(A)  (m 1/2):           5153.506348
Right Ascen at Week(rad):  -0.1138196892E+001
Argument of Perigee(rad):  -0.426857868
Mean Anom(rad):            -0.2825913564E+001
Af0(s):                     0.4634857178E-003
Af1(s/s):                  -0.2546585165E-010
week:                        114

******** Week  114 almanac for PRN-05 ********
ID:                         05
Health:                     000
Eccentricity:               0.3269195557E-002
Time of Applicability(s):  589824.0000
Orbital Inclination(rad):   0.9361980622
Rate of Right Ascen(r/s):  -0.7977475151E-008
SQRT(A)  (m 1/2):           5153.503906
Right Ascen at Week(rad):   0.2966668660E+001
Argument of Perigee(rad):   0.494966090
Mean Anom(rad):            -0.3070877487E+001
Af0(s):                     0.3213882446E-003
Af1(s/s):                   0.0000000000E+000
week:                        114

******** Week  114 almanac for PRN-06 ********
ID:                         06
Health:                     000
Eccentricity:               0.6754875183E-002
Time of Applicability(s):  589824.0000
Orbital Inclination(rad):   0.9429152203
Rate of Right Ascen(r/s):  -0.8034620388E-008
SQRT(A)  (m 1/2):           5153.583984
Right Ascen at Week(rad):  -0.2213439152E+001
Argument of Perigee(rad):  -2.237058187
Mean Anom(rad):            -0.1999352209E+001
Af0(s):                    -0.9536743164E-006
Af1(s/s):                   0.0000000000E+000
week:                        114

******** Week  114 almanac for PRN-07 ********
ID:                         07
Health:                     000
Eccentricity:               0.1203107834E-001
Time of Applicability(s):  589824.0000
Orbital Inclination(rad):   0.9446828935
Rate of Right Ascen(r/s):  -0.7966046104E-008
SQRT(A)  (m 1/2):           5153.732910
Right Ascen at Week(rad):  -0.2243330805E+001
Argument of Perigee(rad):  -1.980474434
Mean Anom(rad):            -0.3469994871E-001
Af0(s):                     0.5636215210E-003
Af1(s/s):                   0.2546585165E-010
week:                        114

******** Week  114 almanac for PRN-08 ********
ID:                         08
Health:                     000
Eccentricity:               0.8266448975E-002
Time of Applicability(s):  589824.0000
Orbital Inclination(rad):   0.9588003104
Rate of Right Ascen(r/s):  -0.8000333246E-008
SQRT(A)  (m 1/2):           5153.647949
Right Ascen at Week(rad):   0.2008921988E+001
Argument of Perigee(rad):   2.061123773
Mean Anom(rad):            -0.1727268359E+001
Af0(s):                     0.6132125854E-003
Af1(s/s):                   0.1455191523E-010
week:                        114

******** Week  114 almanac for PRN-09 ********
ID:                         09
Health:                     000
Eccentricity:               0.1249456406E-001
Time of Applicability(s):  589824.0000
Orbital Inclination(rad):   0.9449645227
Rate of Right Ascen(r/s):  -0.8160339911E-008
SQRT(A)  (m 1/2):           5153.631348
Right Ascen at Week(rad):   0.1954545065E+001
Argument of Perigee(rad):   0.778354061
Mean Anom(rad):            -0.2282333465E+001
Af0(s):                    -0.1525878906E-004
Af1(s/s):                   0.0000000000E+000
week:                        114

******** Week  114 almanac for PRN-10 ********
ID:                         10
Health:                     000
Eccentricity:               0.4541873932E-002
Time of Applicability(s):  589824.0000
Orbital Inclination(rad):   0.9795390116
Rate of Right Ascen(r/s):  -0.7714607059E-008
```

```
SQRT(A)  (m 1/2):           5153.639160
Right Ascen at Week(rad):  -0.1133894930E+000
Argument of Perigee(rad):   0.069642578
Mean Anom(rad):             0.1240936154E+001
Af0(s):                     0.1335144043E-004
Af1(s/s):                   0.0000000000E+000
week:                        114

******** Week  114 almanac for PRN-11 ********
ID:                         11
Health:                     000
Eccentricity:               0.9374618530E-003
Time of Applicability(s):  589824.0000
Orbital Inclination(rad):   0.9198755479
Rate of Right Ascen(r/s):  -0.8697505143E-008
SQRT(A)  (m 1/2):           5153.635742
Right Ascen at Week(rad):  -0.1217956028E+001
Argument of Perigee(rad):  -2.106351863
Mean Anom(rad):             0.5861712850E+000
Af0(s):                     0.4768371582E-005
Af1(s/s):                   0.0000000000E+000
week:                        114

******** Week  114 almanac for PRN-13 ********
ID:                         13
Health:                     000
Eccentricity:               0.1811027527E-002
Time of Applicability(s):  589824.0000
Orbital Inclination(rad):   0.9704789376
Rate of Right Ascen(r/s):  -0.7623174679E-008
SQRT(A)  (m 1/2):           5153.617676
Right Ascen at Week(rad):   0.9307383490E+000
Argument of Perigee(rad):   0.128367527
Mean Anom(rad):             0.1773525595E+001
Af0(s):                    -0.6675720215E-005
Af1(s/s):                   0.0000000000E+000
week:                        114

******** Week  114 almanac for PRN-14 ********
ID:                         14
Health:                     000
Eccentricity:               0.2154827118E-002
Time of Applicability(s):  589824.0000
Orbital Inclination(rad):   0.9651339733
Rate of Right Ascen(r/s):  -0.7646032774E-008
SQRT(A)  (m 1/2):           5153.636230
Right Ascen at Week(rad):   0.9263289032E+000
Argument of Perigee(rad):  -0.529618477
Mean Anom(rad):            -0.1470162169E+001
Af0(s):                    -0.1220703125E-003
Af1(s/s):                   0.0000000000E+000
week:                        114

******** Week  114 almanac for PRN-15 ********
ID:                         15
Health:                     000
Eccentricity:               0.8009910583E-002
Time of Applicability(s):  589824.0000
Orbital Inclination(rad):   0.9786162263
Rate of Right Ascen(r/s):  -0.8103194673E-008
SQRT(A)  (m 1/2):           5153.595215
Right Ascen at Week(rad):  -0.1092222784E+001
Argument of Perigee(rad):   1.770633652
Mean Anom(rad):            -0.1338743533E+001
Af0(s):                     0.1010894775E-003
Af1(s/s):                   0.3637978807E-011
week:                        114

******** Week  114 almanac for PRN-17 ********
ID:                         17
Health:                     000
Eccentricity:               0.1351499557E-001
Time of Applicability(s):  589824.0000
Orbital Inclination(rad):   0.9805037417
Rate of Right Ascen(r/s):  -0.8091765626E-008
SQRT(A)  (m 1/2):           5153.628418
Right Ascen at Week(rad):  -0.1051987995E+001
Argument of Perigee(rad):  -3.098622841
Mean Anom(rad):            -0.2480314733E+001
Af0(s):                     0.2365112305E-003
Af1(s/s):                   0.8003553376E-010
week:                        114

******** Week  114 almanac for PRN-18 ********
ID:                         18
Health:                     000
Eccentricity:               0.2409934998E-002
Time of Applicability(s):  589824.0000
Orbital Inclination(rad):   0.9623416489
Rate of Right Ascen(r/s):  -0.7840326581E-008
SQRT(A)  (m 1/2):           5153.610840
Right Ascen at Week(rad):  -0.6629635767E-001
Argument of Perigee(rad):   2.880236557
Mean Anom(rad):             0.3060057230E+001
Af0(s):                    -0.7534027100E-004
Af1(s/s):                   0.0000000000E+000
week:                        114

******** Week  114 almanac for PRN-20 ********
ID:                         20
Health:                     000
Eccentricity:               0.2077102661E-002
Time of Applicability(s):  589824.0000
Orbital Inclination(rad):   0.9630187576
Rate of Right Ascen(r/s):  -0.7863184676E-008
SQRT(A)  (m 1/2):           5153.681641
Right Ascen at Week(rad):  -0.1183768031E+000
Argument of Perigee(rad):   2.128426431
Mean Anom(rad):             0.1413885372E+001
Af0(s):                    -0.1115798950E-003
Af1(s/s):                  -0.3637978807E-011
week:                        114

******** Week  114 almanac for PRN-21 ********
ID:                         21
Health:                     000
Eccentricity:               0.1791334152E-001
Time of Applicability(s):  589824.0000
Orbital Inclination(rad):   0.9791914691
Rate of Right Ascen(r/s):  -0.7668890869E-008
SQRT(A)  (m 1/2):           5153.588867
Right Ascen at Week(rad):  -0.1074719074E+000
Argument of Perigee(rad):  -2.398434014
Mean Anom(rad):             0.1499590182E+001
Af0(s):                     0.4768371582E-005
Af1(s/s):                   0.0000000000E+000
week:                        114

******** Week  114 almanac for PRN-22 ********
ID:                         22
Health:                     000
Eccentricity:               0.1473951340E-001
Time of Applicability(s):  589824.0000
Orbital Inclination(rad):   0.9326207711
Rate of Right Ascen(r/s):  -0.8034620388E-008
SQRT(A)  (m 1/2):           5153.560059
Right Ascen at Week(rad):   0.2959023473E+001
Argument of Perigee(rad):   0.725182676
Mean Anom(rad):             0.8577881249E+000
Af0(s):                     0.3881454468E-003
Af1(s/s):                   0.4001776688E-010
week:                        114

******** Week  114 almanac for PRN-23 ********
ID:                         23
Health:                     000
Eccentricity:               0.1575088501E-001
Time of Applicability(s):  589824.0000
Orbital Inclination(rad):   0.9824931230
Rate of Right Ascen(r/s):  -0.7634603726E-008
SQRT(A)  (m 1/2):           5153.344727
Right Ascen at Week(rad):  -0.6499269870E-001
Argument of Perigee(rad):  -1.809501115
Mean Anom(rad):             0.1981789702E+001
Af0(s):                     0.2288818359E-004
Af1(s/s):                   0.0000000000E+000
week:                        114

******** Week  114 almanac for PRN-24 ********
ID:                         24
Health:                     000
Eccentricity:               0.9502887726E-002
Time of Applicability(s):  589824.0000
Orbital Inclination(rad):   0.9822474464
Rate of Right Ascen(r/s):  -0.8080336578E-008
SQRT(A)  (m 1/2):           5153.563477
Right Ascen at Week(rad):  -0.1120960580E+001
Argument of Perigee(rad):  -1.610753605
Mean Anom(rad):            -0.2193915352E+001
Af0(s):                     0.3814697266E-005
Af1(s/s):                   0.3637978807E-011
week:                        114

******** Week  114 almanac for PRN-25 ********
ID:                         25
Health:                     000
```

```
Eccentricity:               0.9082317352E-002
Time of Applicability(s):  589824.0000
Orbital Inclination(rad):   0.9377620036
Rate of Right Ascen(r/s):  -0.8228914196E-008
SQRT(A)  (m 1/2):           5153.750977
Right Ascen at Week(rad):   0.1911440430E+001
Argument of Perigee(rad):  -1.931039131
Mean Anom(rad):            -0.1465604418E+001
Af0(s):                     0.1907348633E-004
Af1(s/s):                   0.0000000000E+000
week:                        114

******** Week  114 almanac for PRN-26 ********
ID:                         26
Health:                     000
Eccentricity:               0.1311683655E-001
Time of Applicability(s):  589824.0000
Orbital Inclination(rad):   0.9691187280
Rate of Right Ascen(r/s):  -0.7646032774E-008
SQRT(A)  (m 1/2):           5153.701172
Right Ascen at Week(rad):   0.9354833530E+000
Argument of Perigee(rad):   0.301388651
Mean Anom(rad):            -0.4329087778E+000
Af0(s):                     0.2861022949E-005
Af1(s/s):                  -0.3637978807E-011
week:                        114

******** Week  114 almanac for PRN-27 ********
ID:                         27
Health:                     000
Eccentricity:               0.1542854309E-001
Time of Applicability(s):  589824.0000
Orbital Inclination(rad):   0.9422860485
Rate of Right Ascen(r/s):  -0.8183198006E-008
SQRT(A)  (m 1/2):           5153.588867
Right Ascen at Week(rad):   0.1935252710E+001
Argument of Perigee(rad):  -2.530072860
Mean Anom(rad):            -0.2927130455E+001
Af0(s):                     0.9536743164E-006
Af1(s/s):                   0.0000000000E+000
week:                        114

******** Week  114 almanac for PRN-28 ********
ID:                         28
Health:                     000
Eccentricity:               0.5639076233E-002
Time of Applicability(s):  589824.0000
Orbital Inclination(rad):   0.9598609143
Rate of Right Ascen(r/s):  -0.7703178011E-008
SQRT(A)  (m 1/2):           5153.620605
Right Ascen at Week(rad):   0.3026213779E+001
Argument of Perigee(rad):  -2.478347448
Mean Anom(rad):             0.1726786743E+001
Af0(s):                    -0.3433227539E-004
Af1(s/s):                  -0.3637978807E-011
week:                        114

******** Week  114 almanac for PRN-29 ********
ID:                         29
Health:                     000
Eccentricity:               0.8531570435E-002
Time of Applicability(s):  589824.0000
Orbital Inclination(rad):   0.9660327901
Rate of Right Ascen(r/s):  -0.7634603726E-008
SQRT(A)  (m 1/2):           5153.862793
Right Ascen at Week(rad):   0.9059152741E+000
Argument of Perigee(rad):  -1.865944941
Mean Anom(rad):            -0.5308584695E+000
Af0(s):                     0.6151199341E-003
Af1(s/s):                  -0.3637978807E-011
week:                        114

******** Week  114 almanac for PRN-30 ********
ID:                         30
Health:                     000
Eccentricity:               0.5998611450E-002
Time of Applicability(s):  589824.0000
Orbital Inclination(rad):   0.9433406603
Rate of Right Ascen(r/s):  -0.7874613724E-008
SQRT(A)  (m 1/2):           5153.576172
Right Ascen at Week(rad):   0.3001437892E+001
Argument of Perigee(rad):   1.343137624
Mean Anom(rad):             0.1789605429E+001
Af0(s):                     0.1335144043E-003
Af1(s/s):                   0.1818989404E-010
week:                        114

******** Week  114 almanac for PRN-31 ********
ID:                         31
Health:                     000
Eccentricity:               0.1043844223E-001
Time of Applicability(s):  589824.0000
Orbital Inclination(rad):   0.9441316191
Rate of Right Ascen(r/s):  -0.7988904198E-008
SQRT(A)  (m 1/2):           5153.647461
Right Ascen at Week(rad):  -0.2243438289E+001
Argument of Perigee(rad):   0.866585670
Mean Anom(rad):            -0.1029626930E+001
Af0(s):                     0.7343292236E-004
Af1(s/s):                   0.3637978807E-011
week:                        114
```

A.2 OCL Script Files for Extraction of Simulation Data

A tabular ephemeris of the simulated spacecraft trajectory in comma separated (CSV) format for easy import into common spreadsheet programs is obtained from the LEO__ECEF.OCL script:

```
![header]
!Tabulation of spacecraft ECEF position and velocity
![command]
!START_TIME 0
!STOP_TIME 1500
STEP_SIZE 1
TABULATE "LEO_ECEF"
COMMA_SEPARATED
PARAMETER SIM_TIME    "TIME"
PARAMETER RT_ANT_X     "POS_X"
PARAMETER RT_ANT_Y     "POS_Y"
PARAMETER RT_ANT_Z     "POS_Z"
PARAMETER RT_ANT_X_VEL "VEL_X"
PARAMETER RT_ANT_Y_VEL "VEL_Y"
PARAMETER RT_ANT_Z_VEL "VEL_Z"
END_TABULATE
EXIT
```

Simulated pseudoranges for all satellites may be extracted using the LEO__PR.OCL script:

```
![header]
!Tabulation of pseudoranges
![command]
STEP_SIZE  1
TABULATE "LEO_PR"
COMMA_SEPARATED
PARAMETER SIM_TIME    "TIME"
PARAMETER RT_SAT_PSEUDORANGE@SAT1.     "PR#1 "
PARAMETER RT_SAT_PSEUDORANGE@SAT2      "PR#2 "
…
PARAMETER RT_SAT_PSEUDORANGE@SAT31     "PR#31"
PARAMETER RT_SAT_PSEUDORANGE@SAT32     "PR#32"
END_TABULATE
EXIT
```

Pseudorange rates for all satellites can be obtained from the LEO__PRR.OCL script:

```
![header]
!Tabulation of pseudorangerates
![command]
STEP_SIZE  1
TABULATE "LEO_PRR"
COMMA_SEPARATED
PARAMETER SIM_TIME    "TIME"
PARAMETER RT_SAT_PR_RATE@SAT1.     "PRR#1 "
PARAMETER RT_SAT_PR_RATE@SAT2      "PRR#2 "
…
PARAMETER RT_SAT_PR_RATE@SAT31     "PRR#31"
PARAMETER RT_SAT_PR_RATE@SAT32     "PRR#32"
END_TABULATE
EXIT
```

A.3 Exchanging Scenario Definitions between Simulators

The Spirent signal simulators employ various types of VMS file formats that cannot be recovered properly when transferring these files via intermediate DOS or Unix file systems. As a workaround, files can be packed using a VMS specific version of the ZIP/UNZIP utility that is provided with the simulator. It allows storage of VMS version numbers and file attributes as part of the archive. Unless configured by the provider the two programs can be made accessible by defining the DCL symbols:

```
$ ZIP==$SYS$SYSDEVICE:[GPS.V680.UNSC]ZIP.EXE
$ UNZIP==$SYS$SYSDEVICE:[GPS.V680.UNSC]UNZIP.EXE
```

Before creating a zip archive it is suggested[6] to copy the scenario file and the source files required from the source data directory to a temporary directory on the Alpha:

```
$ SET DEF GPS$DATA
$ CREATE/DIR [.TEMP]
$ COPY scenario_name.SCEN;version_number [.TEMP]*.*;*
$ COPY source_file.extension;version_number [.TEMP]*.*;*
$ …
```

The last line is repeated until all the necessary files (i.e. all the files listed in the EDIT SOURCE FILES window) are copied for the scenario. After changing to the temporary directory SYS$SYSDEVICE:[GPSSIM.DATA.TEMP] using

```
$ SET DEF [.TEMP]
$ SH DEF
```

the archive is created using the command

```
$ ZIP "-Vw" SCENS.ZIP *.*;* -i *.*;*
```

This file (scens.zip) can now be safely transferred by a BINARY mode (IMAGE) FTP to a PC and E Mail etc. After transfer to the GPS$DATA directory on the destination Alpha by BINARY (Image) FTP the archive is extracted using:

```
$ UNZIP "-V" SCENS.ZIP
```

The ZIP/UNZIP must be used with switches as given above to preserve the VMS structure and attributes.

To transfer the zipped scenarios to an MS-DOS formatted floppy disk using the simulator's built-in disk drive, the OpenVMS PCDISK utility is required. A typical session log is given below:

```
$ PCDISK
PCDISK> USE A: DVA0:
A:> IMPORT SCENS.ZIP;1 A:\SCENS.ZIP
A:> EXIT
```

Vice versa, the EXPORT command can be used to read a scenario from the disk:

```
$ PCDISK
PCDISK> USE A: DVA0:
A:> EXPORT A:\SCENS.ZIP SCENS.ZIP;1
A:> EXIT
```

[6] Private communication A. Proctor, SPIRENT, 5 April 2002